Paper SAS3341-2019

Medical Image Analytics in SAS® Viya® with Applications in the Treatment of Colorectal Cancer Spread to the Liver

Fijoy Vadakkumpadan and Joost Huiskens, SAS Institute Inc.

ABSTRACT

The powerful analytics in SAS® Viya® have been recently extended to include the ability to process medical images, the largest driver of health-care data growth. This new extension, released in SAS® Visual Data Mining and Machine Learning 8.3 in SAS® Viya® 3.4 enables customers to load, visualize, analyze, and save health-care image data and associated metadata at scale. As SAS continues to build on this foundation, several substantially new medical image processing capabilities are planned for future versions of SAS Visual Data Mining and Machine Learning. In particular, these new capabilities will enable customers to perform the following tasks: process generic data files, such as radiotherapy (DICOM-RT) files, under the Digital Imaging and Communications in Medicine (DICOM) standard; process images in a single SAS® Cloud Analytic Services (CAS) action call even when the processing parameters vary from one image to another in the input table; use highly advanced techniques to perform image segmentation; and quantify the size and shape of tissue regions in binary images. This paper demonstrates the new capabilities by applying them to colorectal liver metastases (CRLM) morphometry with computed tomography (CT) scans to assess patients' response to chemotherapy. This study is a collaborative effort between SAS and Amsterdam University Medical Center (AUMC) for improving CRLM treatment strategies.

INTRODUCTION

Imaging has been revolutionizing medicine for decades. From simple 2-D X-rays at the dentist's office to exquisite 4-D ultrasounds of a baby in its mother's womb, it has touched and saved countless lives. Physicians routinely rely on image-based data to diagnose diseases, guide therapeutic procedures, and monitor patients' response to treatment. The benefits of these imaging technologies come with a hefty price, however, since medical image data are notoriously large. As of 2016, over 600 million imaging procedures were performed annually in the US alone, generating millions of terabytes of data. This constitutes over 90% of total health-care data, making imaging the largest driver of health-care data growth. To make matters worse, the extraction of relevant information from medical images, for example, the boundaries of tumors, is typically done manually by health-care professionals using a labor-intensive and subjective process. The sheer volume of the data combined with the extensive cognitive input required for its processing make it extremely challenging for the health-care industry to convert the images into objective insights that can drive decisions. Further, as the volume of medical imaging data continues to rise, radiologists are subject to excessive cognitive workloads, which leads to fatigue and increased risk of medical errors. A typical radiologist combs through thousands of images in a single day, as he or she examines tens of patients, each with hundreds of cross-sectional image slices. Therefore, any automated assistance offered to the radiologists can dramatically improve their lives and the quality of the health care their patients receive.

SAS has a rich history of supporting health and life sciences customers for their clinical data management, analytics, and compliance needs. SAS® Analytics provides an integrated environment for collection, classification, analysis, and interpretation of data to reveal patterns, anomalies, and key variables and relationships, leading ultimately to new insights for guided decision-making. The application of SAS® algorithms has enabled patients to transform themselves from being passive recipients to becoming active participants in their own personalized health care. With the release of SAS® Viya® 3.4, SAS customers can now

extend the analytics framework to take advantage of medical images along with statistical, visualization, data mining, text analytics, and optimization techniques for better clinical diagnosis. Images are supported as a standard SAS data type in SAS® Visual Data Mining and Machine Learning, which offers an end-to-end visual environment for machine learning and deep learning—from data access and data preparation to sophisticated model building and deployment in a scalable distributed framework. It provides a comprehensive suite of programmatic actions to load, visualize, process, and save health-care image data and associated metadata at scale in formats such as Digital Imaging and Communication in Medicine (DICOM), Neuroimaging Informatics Technology Initiative (NIfTI), nearly raw raster data (NRRD), and so on.

The goal of this paper is twofold. First, it provides a comprehensive overview of end-to-end medical image analytics capabilities in SAS® Visual Data Mining and Machine Learning in SAS Viya, with special focus on future releases of this product. Second, it illustrates these capabilities by working through a real-world, clinically significant use case that is part of a collaboration between SAS and Amsterdam University Medical Center (AUMC) aimed at improving treatment strategies for patients with colorectal cancer spread to the liver, known as colorectal liver metastases (CRLM).

END-TO-END BIOMEDICAL IMAGE ANALYTICS IN SAS VIYA

SAS Viya uses an analytic engine known as SAS Cloud Analytic Services (CAS) to perform various tasks, including medical image analytics. Building end-to-end solutions in SAS Viya typically involves assembling CAS actions, which are the smallest units of data processing that are initiated by a CAS client on a CAS server. CAS actions are packaged into logical groups called action sets. At this time, two action sets, Image and BioMedImage, host actions that directly operate on medical imagery.

The Image action set contains two actions that directly operate on medical image imagery: the loadImages action loads biomedical images from disk into memory, and the saveImages action saves the loaded images from memory to disk. These actions support all common biomedical image formats, including the DICOM standard, which is widely used in clinical settings. The BioMedImage action set currently includes three actions, processBioMedImages, segmentBioMedImages, and buildSurface, with two new actions, loadDicomData and quantifyBioMedImages, to be added in future releases. The loadDicomData action is for loading generic DICOM files, including non-image files, into memory. The other actions facilitate preprocessing, segmentation, visualization, and quantification of medical images. At this time, full support is available only for two- and three-dimensional (2-D and 3-D), single-channel medical images in these action sets.

The output produced by some of the actions in the Image and BioMedImage action sets can be used as input to other actions, such as those in action sets for traditional machine learning (ML) and deep learning (DL), to derive insights that inform decisions. Figure 1 presents an end-to-end biomedical image analytics pipeline in SAS Viya. On one end of the pipeline are raw image data and metadata on disk, and on the other end are helpful insights that can inform decisions. The major steps in the pipeline, along with the primary action sets (in italics) that can be used to implement those steps, are displayed in rectangular boxes. The examples of ML and DL action sets include the RobustPCA action set, which performs principal component analysis (PCA), and the DeepLearn action, which performs deep learning. Steps in which new actions or major upgrades to existing actions will be available in upcoming releases of SAS® Visual Data Mining and Machine Learning are highlighted in red. The green arrows signify critical features available in future releases of the Image and BioMedImage action sets to facilitate the use of generic data processing action sets such as DataStep and FedSQL to process tables containing image data. These generic action sets are critical to integrating binary image-based data from various sources

and to processing non-binary image-based metadata while retaining the corresponding binary image-based data.

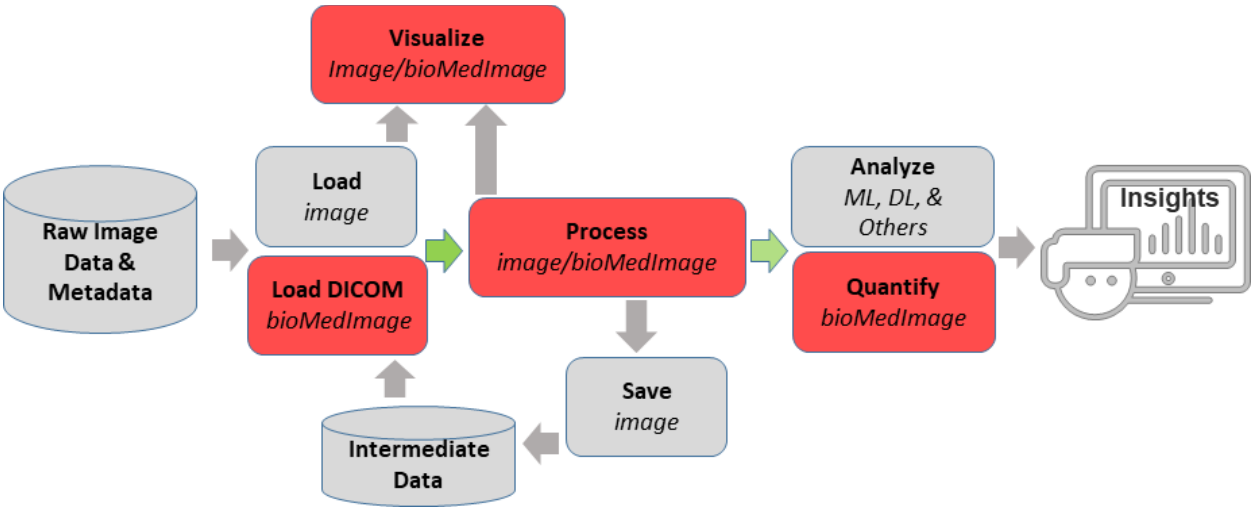

Figure 1. Processing Pipeline for End-to-End Biomedical Image Analytics in SAS Viya

CRLM MORPHOMETRY: AN EXAMPLE USE CASE

This section provides an example for the pipeline shown in Figure 1 by demonstrating how to build an end-to-end solution that can assist with a real-world biomedical image analytics problem, specifically assessment of therapy response in patients with CRLM, based on 3-D computed tomography (CT) images of the patients' torsos. Colorectal cancer is the third most common cancer and the second leading cause of cancer-related deaths worldwide (Bray et al. 2018). Most cancer deaths are the result of progression of metastases, that is, spreading of the cancer. Approximately 50% of colorectal cancer patients will develop metastases to the liver (Donadon et al. 2007). Patients with liver-only colorectal metastases can be treated with curative intent. Complete surgical resection of CRLM is considered the only chance for cure for these patients (Angelsen et al. 2017). Initially unresectable liver metastases can become resectable after downsizing of the lesions by systemic therapy, the main component of which is chemotherapy (Lam et al. 2012). However, there is no consensus regarding the optimal systemic therapy regime.

Accordingly, assessment of patient response to treatment is a crucial feature in the clinical evaluation of systemic therapy. The widely accepted and applied criterion for such assessment is the Response Evaluation Criteria In Solid Tumors (RECIST), which aims to measure the objective change of anatomical tumor size (Eisenhauer et al. 2009). The RECIST assessment is performed by measuring changes in one-dimensional (1-D) diameter of two target lesions before and after therapy. Though RECIST is a clinical standard worldwide, it is highly limited. Firstly, its measurement is manual and labor intensive. Secondly, it is very subjective, as the target lesions, image slices for measurement, and the line segment for lesion diameter measurement are all selected by a radiologist subjectively (Yoon et al. 2016). Finally, RECIST ignores the exquisite 3-D and gray-scale information provided by modern CT scanners. Some of this information has been proven to be significantly associated with pathologic response and overall survival in patients with CRLM (Chun et al. 2009).

This paper demonstrates the medical image analytics capabilities of SAS Viya by using the SAS® Platform to compute new criteria that can potentially assist radiologists with improving assessment of CRLM treatment response. Two different approaches, one based on semi-automatic image segmentation, and the other on automatic object detection with

deep learning, are demonstrated. All client-side source code in this demonstration was written in Python. The SAS Scripting Wrapper for Analytics Transfer (SWAT) package was used to interface with the CAS server, and the Mayavi library (Ramachandran and Varoquaux 2011) was used to perform 3-D visualizations of image-based data.

DATA SELECTION AND PREPROCESSING

All patient data used in this paper was collected as part of the Treatment Strategies in Colorectal Cancer Patients with Initially Unresectable Liver-Only Metastases (CAIRO5) clinical trial (Huiskens et al. 2015) and provided by AUMC. The data consisted of 3-D, abdominal and thoracic transaxial CT images of patients in DICOM format (Figure 2A), and expert radiologist segmentations of liver and lesions in each scan. The in-plane pixel size of the images ranged from 0.6 to 0.8 mm, and the slice thickness ranged from 3 to 5 mm. The expert segmentations were performed semi-automatically using the Philips IntelliSpace Portal software at AUMC, and the resulting 3-D organ contours were stored as DICOM radiotherapy (DICOM-RT) files (Figure 2B). Each patient received a baseline scan before therapy and regular follow-up scans throughout therapy. Most patients received one follow-up scan, with some receiving two. Since the goal of this paper is to demonstrate the capabilities of SAS Viya and not to statistically show clinical significance, only a small set of 10 patients was included in the analyses.

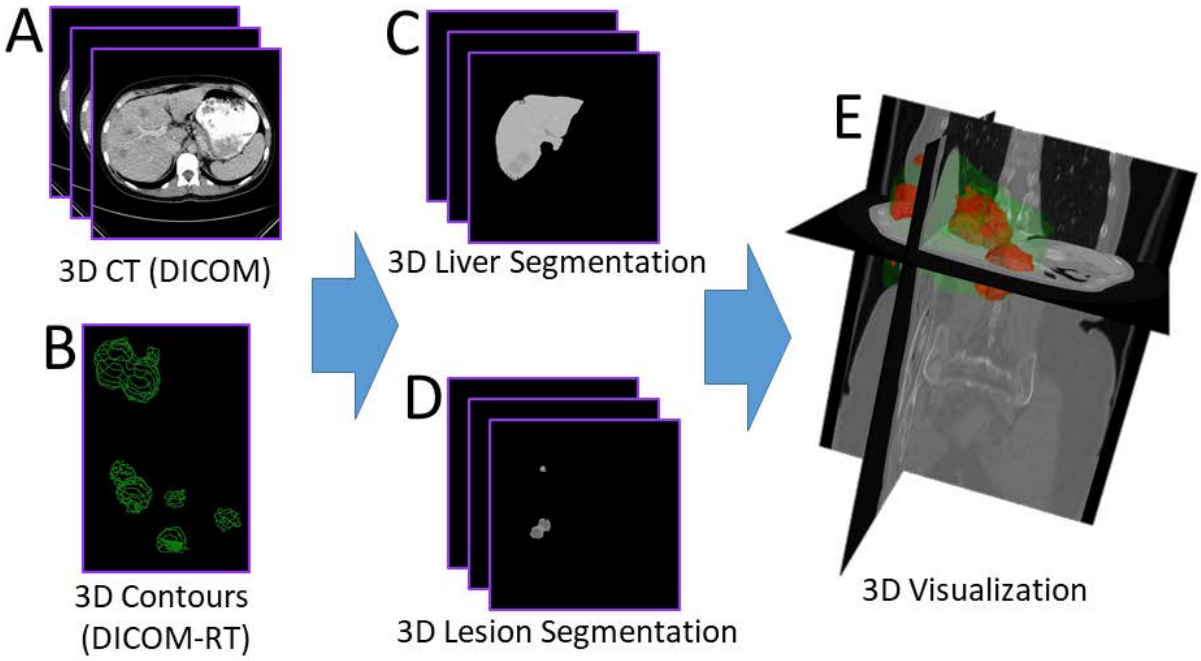

Figure 2. Steps in Data Processing

To preprocess the data, all 3-D images were recursively loaded on the CAS server as illustrated by this code snippet:

```
# DICOM Keywords for images
imsuid = 'SeriesInstanceUID'
impn = 'PatientName'
imad = 'AcquisitionDate'
impa = 'PatientAge'
impx = 'PatientSex'
all_keys_im = [imsuid, impn, imad, impa, impx]
```

```
# Load the DICOM series
imdata = s.CASTable(name='imdata_orig', replace=True)
r = s.image.loadimages(
    path='AUMCImages',
    casOut=imdata,
    recurse=True,
    addcolumns=dict(
        general={'position', 'orientation', 'spacing'},
        dicomattributes=dict(keywords=all_keys_im)),
    series=dict(dicom=True),
    decode=True
)
```

Note that several DICOM attributes of each image, including `SeriesInstanceUID`, were loaded by specifying the `dicomattributes` parameter. Next, the DICOM-RT data were loaded as follows:

```
# DICOM keywords for RT data
rtsuid =
'ReferencedFrameOfReferenceSequence{1}RTReferencedStudySequence{1}RTReferen
cedSeriesSequence{1}SeriesInstanceUID'
rtcsq = 'ROIContourSequence'
rtsdesc = 'SeriesDescription'
all_keys_rt = [rtsuid, rtcsq, rtsdesc]

# Call the new loadDicomData
rtdata = s.CASTable(name='rtdata', replace=True)
r = s.biomedimage.loaddicomdata(
    path='AUMCDicomRt/',
    casOut=rtdata,
    addColumns=dict(keywords=all_keys_rt)
)
```

Here, loadDicomData is an action that will be available in future releases of SAS Visual Data Mining and Machine Learning in the BioMedImage action set. This action can load user-provided attributes from DICOM files in a given directory or file path, including nested sequence attributes. For example, the attribute specified by the variable `rtsuid` in the above snippet specifies multiple nesting levels to access the DICOM series universal identifier (UID) of the image that corresponds to each DICOM-RT file being loaded.

The next step was to merge imdata, the table containing the images, with rtdata, the table containing DICOM-RT data, by using the DataStep action set in CAS, as follows:

```
# Function to convert strings into column names
def col(s):
    s = str.replace(str.replace(s, '{', '_'), '}', '_')
    return '_'+s+'_'

# Create views in preparation for data step
r = s.table.view(
    name='rtview',
    tables=[dict(name='rtdata',
        computedvars={'vccsq', 'suid', 'rtid'},
        computedvarsprogram=
            "length vccsq varchar(*); vccsq="+col(rtcsq)+";"
            "length suid varchar(64); suid="+col(rtsuid)+";"
            "rtid=_id_;",
        varlist={col(rtsdesc)})],
```

```
    replace=True)

r = s.table.view(
    name='imview',
    tables=[dict(name='imdata_orig',
        where='_depth_>1',
        computedvars={'vcimage', 'vcres', 'vcpos', 'vcori', 'vcspa',
                      'adate', 'suid'},
        computedvarsprogram=
            "length vcimage varchar(*); vcimage=_image_;"
            "length vcres varchar(24); vcres=_resolution_;"
            "length vcpos varchar(24); vcpos=_position_;"
            "length vcori varchar(72); vcori=_orientation_;"
            "length vcspa varchar(24); vcspa=_spacing_;"
            "length suid varchar(64); suid="+col(imsuid)+";"
            "adate=input("+col(imad)+", yymmdd8.);",
        varlist={'_id_', '_dimension_', '_imageFormat_', col(impn)})],
    replace=True)

# Merge the tables on DICOM series UID
r = s.datastep.runcode(code="data imrt;"
                       "merge imview(in=a) rtview(in=b);"
                       "by suid;"
                       "if a & b;"
                       "run;")
```

Note that the runCode action in the DataStep action set was performed on views of the image data tables generated by the view action in the table action set, and not directly on the tables. This is because the tables contained binary data columns of type varbinary, such as _image_, which the runCode action does not currently support. The views helped cast the binary data as the character type varchar, which runCode supports. To facilitate processing of the table produced by runCode, actions in the BioMedImage action set have been updated to accept columns of type varchar also for variables where it previously required varbinary columns.

Three-dimensional images of liver (Figure 2C) and lesion (Figure 2D) segmentations were then generated by processing the merged table with the processBioMedImages action in the BioMedImage action set, like so:

```
masks = s.CASTable(name='masks', replace=True)
imrt = s.CASTable(name='imrt', replace=True)
s.biomedimage.processbiomedimages(
    images=dict(table=imrt, image='vcimage',
           resolution='vcres',
           position='vcpos',
           orientation='vcori',
           spacing='vcspa'),
    steps=[dict(stepparameters=dict(steptype='roi2mask',
        roi2maskparameters=dict(roi2masktype='dicomrt_specific',
            roicontoursequence='vccsq',
            pixelintensity='image')))],
    casout=masks,
    decode=True,
    copyvars={'_SeriesDescription_'},
    addcolumns={'position', 'orientation', 'spacing'}
)
```

Here, roi2mask is a new step that will be available in future releases of the processBioMedImages action. This step is capable of processing image-specific DICOM-RT

contour data, as indicated by the 'dicomrt_specific' value of the roi2masktype parameter. The value of 'image' given to the pixelintensity parameter directed the action to retain gray-scale values of pixels that belong to the regions delineated by the DICOM-RT contours. The liver and lesion segmentations generated by the processBioMedImages action can be fed into the buildSurface action in the BioMedImage action set to reconstruct highly detailed surfaces of liver and lesions for 3-D visualization. One such visualization presented in Figure 2E illustrates the exquisite 3-D detail captured by the data used in this paper.

CRITERIA USING IMAGE SEGMENTATION

To compute new criteria in assessing CRLM response that overcome some of the limitations of RECIST, quantifyBioMedImages, a new action that will be available in future releases of SAS® Visual Data Mining and Machine Learning in SAS Viya, was applied to the lesion segmentation images generated in the previous section. This action can compute user-specified quantities or metrics from images. The code to invoke this action was as follows:

```
qdata = s.CASTable(name='qdata', replace=True)
s.biomedimage.quantifybiomedimages(
    images=dict(table=masks.query("find(_SeriesDescription_, 'seg')>0")),
    region='component',
    quantities=[dict(quantityparameters=dict(quantitytype='mean')),
                dict(quantityparameters=dict(quantitytype='content'))],
    labelparameters=dict(labeltype='basic', connectivity='face'),
    casout=qdata)
```

The quantities specified above are mean and content, which directed the action to compute mean CT intensity and volume of each lesion region. Note, the masks table was filtered using information contained in one of the DICOM attributes to select only the lesion segmentation images for these calculations. Also, the combination of region and labelparameters options directed the action to compute the quantities for each connected component (Johnson, McCormick, and Ivanez 2015); that is, lesion region, of each image. The result of the quantifyBioMedImages action was then further processed with the summary action in the Simple action set to compute the total lesion volume and mean lesion intensity of each lesion in each scan of each patient. The results are summarized in Figure 1. Scans 0, 1, and 2 referred to in the legend of the figure were the baseline, first follow-up, and second follow-up scans, respectively. Overall, both the lesion volumes and the mean lesion intensities decreased over therapy. Note that the unit for mean lesion intensity is the Hounsfield unit (HU), the unit of pixel values in CT images.

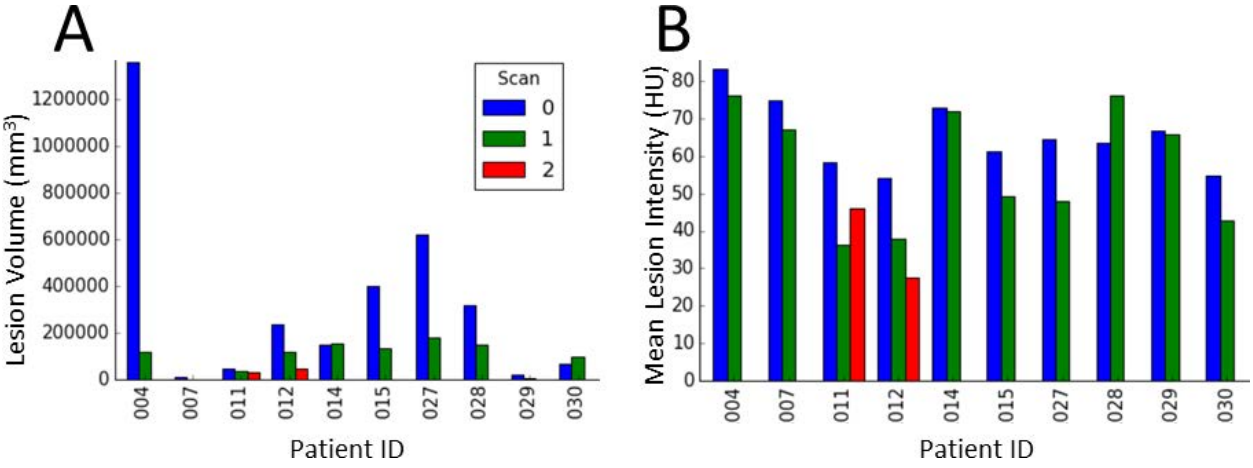

Figure 3. Total Lesion Volumes and Mean Lesion Intensities for Each Scan of Each Patient

CRITERION USING AUTOMATIC OBJECT DETECTION WITH DEEP LEARNING

This section demonstrates preliminary efforts toward using a convolutional neural network-based deep learning object detection model to develop an objective, fully automated surrogate for the RECIST criterion. To prepare the data needed to train the model, the 3-D lesion segmentation images (Figure 4A) were split into individual 2-D slices (Figure 4B) using the export_photo step of the processBioMedImages action in the BioMedImage action set (Vadakkumpadan and Sethi 2018). Then, the bounding box for each 2-D lesion region of each slice was computed (Figure 4C) using the quantifyBioMedImages action, as follows:

```
bbdata = s.CASTable(name='bbdata', replace=True)
s.biomedimage.quantifybiomedimages(
    images=dict(table=masks_exp),
    region='component',
    quantities=[dict(quantityparameters=dict(quantitytype='boundingbox'))],
    labelparameters=dict(labelType='basic', connectivity='face'),
    casout=bbdata)
```

Here, the masks_exp table contained the 2-D slices (Figure 4B). The output table containing the bounding boxes was then merged with corresponding slices from the original 3-D DICOM image (Figure 2A). The merged table contained about 900 rows, each row containing an image slice from one of the 10 patients and bounding boxes of lesions in that slice. Note that only those slices with at least one lesion region was included in this data. These data was then randomly split into training and testing sets of approximately equal size. The YOLOv2 model available in SAS® Visual Data Mining and Machine Learning in SAS Viya was then optimized using the training set to detect CRLM lesions.

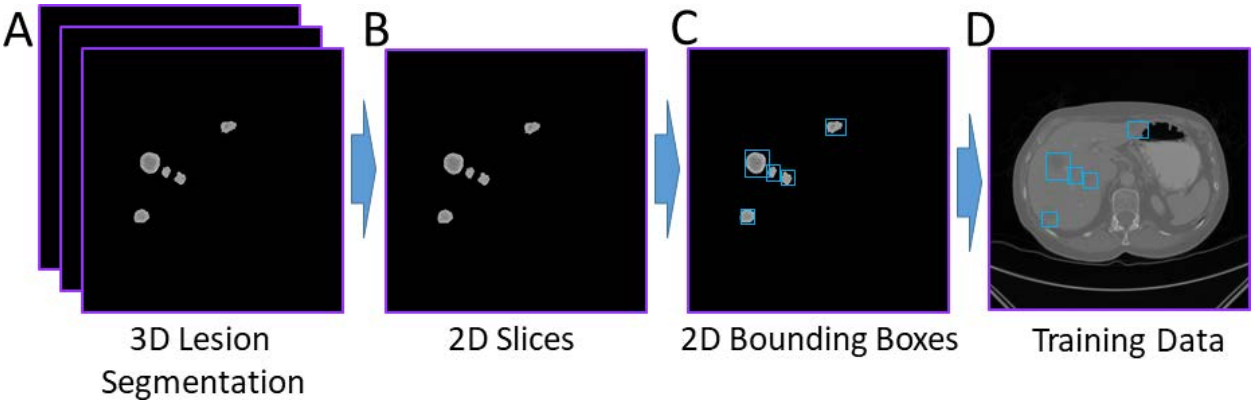

Figure 4. Data Preparation for Training the YOLOv2 Deep Learning Object Detection Model

The model was then scored with the testing set, and the automatically detected lesions were visually examined using the extractDetectedObjects action in the Image action set (Figure 5). It was evident that the model was learning to detect the lesions. At the same time, the model was not perfect, since it missed many lesions, for example, those pointed to by the yellow arrows inFigure 5. To compute a single lesion size metric for each 3-D patient scan, for each detected 2-D bounding box in that scan, the volume of a disc with diameter equal to the average side length the bounding box and thickness equal to the scan's slice thickness was calculated. The volumes of all such discs were then totalled, and the diameter of a sphere with volume equal to this sum was computed. Figure 6 presents this new automatic lesion size metric for each scan of each patient. It is clear from the figure that this new metric captures the reduction in lesion size over therapy, and therefore can be an objective, fully automated surrogate for the RECIST criterion. Note that two of the scans, specifically scan 2 of patient 11 and scan 1 of patient 29, are missing in this plot. This is because the deep learning model failed to detect any lesions in those scans.

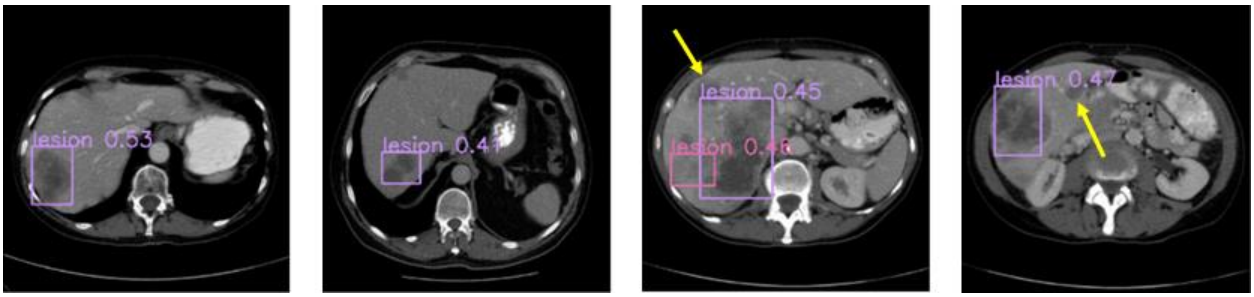

Figure 5. Examples Results from Automatic Detection of CRLM Lesions Using the YOLOv2 Model in This Paper

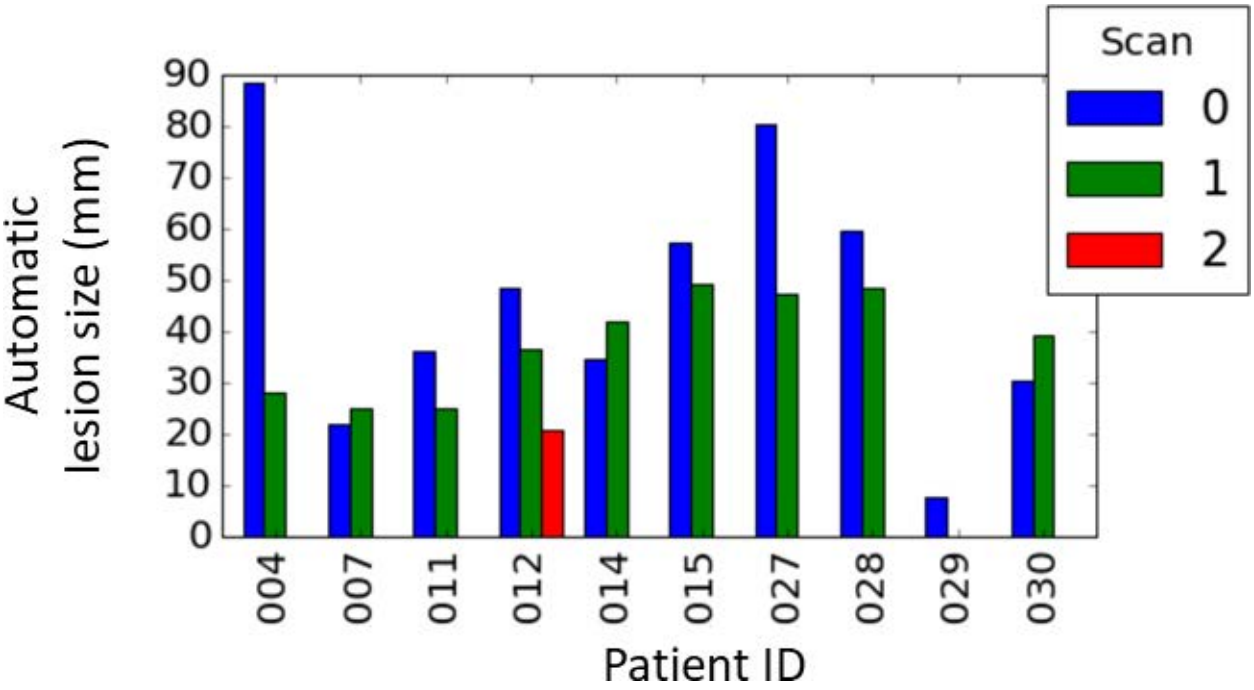

Figure 6. Results from Automatic Lesion Size Measurement Using YOLOv2 Object Detection

DISCUSSION

This paper describes the various SAS Viya components for medical image analytics and to provide illustrations of how to assemble those components to solve real-world problems. Two CAS action sets, Image and BioMedImage, currently host all actions that directly operate on medical imagery. CRLM treatment response assessment is used as an example to illustrate how to assemble these actions in combination with other SAS Viya actions to build complex pipelines that convert raw medical image data and annotations into insights that can help address clinically significant problems. Two image analytic approaches, one using semi-automatic image segmentation and the other using automatic object detection with deep learning, are demonstrated.

The CRLM response assessment metrics presented in this paper can potentially overcome important limitations of the RECIST criterion. The focus of the semi-automatic segmentation approach was to incorporate information ignored by RECIST, while that of the object detection method was to provide a criterion that was fully automated and objective. Specifically, the former approach used the 3-D (Figure 2A) and gray-scale (Figure 4B) information from all lesion regions. In contrast, RECIST is restricted to the usage of simple 1-D diameter measurements made on two target lesions. The object detection approach

provided a lesion size measure (Figure 6) similar to RECIST, but without the subjectivity or labor that is part of RECIST. Such an objective and automated approach, when implemented in a clinic, will help radiologists use their time efficiently and make more consistent decisions across patients. Our preliminary analyses have found quantitative evidence demonstrating that the criteria presented in this paper strongly correlate with, and contain information complementary to, the RECIST measure. These analyses are, however, beyond the scope of this paper and therefore will be published elsewhere.

The CRLM response criteria presented in this paper have some limitations. First, the image segmentation approach involves labor-intensive delineations of the liver and lesion regions from 3-D CT images. However, this limitation will be overcome in the future by using deep U-net style deep learning models (Christ et al. 2016) that will be available in future releases of SAS® Visual Data Mining and Machine Learning. Training of such models was the primary purpose of expert delineations of the liver. Second, the YOLOv2 model used in the object detection approach had limited accuracy. But achieving highly accurate lesion detection was not the goal in this paper. The objective for the model was to attain an accuracy that was sufficient to provide a metric that strongly correlated with the RECIST criterion. Finally, the images in the testing set used to evaluate YOLOv2 deep learning model in this paper strongly correlated with those in the training set since slices from the same 3-D image were included in both sets. However, the goal of this paper was to describe the medical image analytics component of SAS Viya and to demonstrate its potential for solving a clinically significant image analytics problem. The goal was not to develop a model that can be deployed in the clinic.

CONCLUSION

The medical image analytics extension of SAS Viya, available in SAS® Visual Data Mining and Machine Learning, enables customers to load, visualize, process, and save health-care image data and associated metadata at scale. Specific examples provided in this paper demonstrate how the new action sets, when combined with other data analytic capabilities available in SAS Viya, such as deep learning, empowers customers to assemble end-to-end solutions to significant, image-based health-care problems. Upcoming releases of SAS Viya will build on the foundation that this paper demonstrates. These future development efforts will include additional capabilities to process images with image-specific parameters, and to compute more complex quantities from images such as histograms. Also, the BioMedImage action set will be expanded by adding dedicated actions that perform binary operations on images, such as addition and masking.

REFERENCES

Angelsen, J. H., et al. 2017. "Population-based study on resection rates and survival in patients with colorectal liver metastasis in Norway." *The British Journal of Surgery*, 104(5):580-589.

Bray, F., et al. 2018. Global cancer statistics 2018: GLOBOCAN estimates of incidence and mortality worldwide for 36 cancers in 185 countries. *CA Cancer J Clin*, 68(6):394-424.

Christ, P. F., et al. 2016. "Automatic Liver and Lesion Segmentation in CT Using Cascaded Fully Convolutional Neural Networks and 3D Conditional Random Fields." In *Medical Image Computing and Computer-Assisted Intervention – MICCAI 2016*, ed. Ourselin, S., et al, 415-423. Cham: Springer.

Chun, Y. S., et al. 2009. "Association of computed tomography morphologic criteria with pathologic response and survival in patients treated with bevacizumab for colorectal liver metastases." *JAMA*, 302(21):2338-2344.

Donadon M. et al. 2007. "New paradigm in the management of liver-only metastases from colorectal cancer." *Gastrointestinal Cancer Research*, 1(1):20-27

Eisenhauer E.A., et al. 2009. "New response evaluation criteria in solid tumours: revised RECIST guideline (version 1.1)." *European J Cancer*, 45(2):228-247.

Huiskens J., et al. 2015. Treatment strategies in colorectal cancer patients with initially unresectable liver-only metastases, a study protocol of the randomised phase 3 CAIRO5 study of the Dutch Colorectal Cancer Group (DCCG)." *BMC Cancer*, 15:365.

Johnson, H. J., M. McCormick, and L. Ivanez. 2015. The ITK Software Guide Book 1: Introduction and Development Guidelines – Volume 1. New York: Kitware, Inc.

Lam, V. W., et al. 2012. "A systematic review of clinical response and survival outcomes of downsizing systemic chemotherapy and rescue liver surgery in patients with initially unresectable colorectal liver metastases." *Ann Surg Oncol*, 19(4):1292-1301.

Ramachandran, P., and G. Varoquaux. 2011. "Mayavi: 3D Visualization of Scientific Data." *IEEE*, 13(2):40-51.

Vadakkumpadan, F., and S. Sethi. 2018. "Biomedical Image Analytics Using SAS® Viya®." *Proceedings of the SAS Global Forum 2018 Conference*. Cary, NC: SAS Institute Inc. Available https://www.sas.com/content/dam/SAS/support/en/sas-global-forum-proceedings/2018/1961-2018.pdf.

Yoon, S. H., et al. 2016. "Observer variability in RECIST-based tumour burden measurements: a meta-analysis." *Eur J Cancer*, 53:5-15.

ACKNOWLEDGMENTS

We thank Dr. Geert Kazemier at AUMC for providing us with the image data, and Dr. Nina Wesdorp at AUMC for annotating the images.

RECOMMENDED READING

- *SAS® Visual Data Mining and Machine Learning 8.3: Programming Guide*

CONTACT INFORMATION

Your comments and questions are valued and encouraged. Contact the authors at:

Fijoy Vadakkumpadan
SAS Institute, Inc.
+1 919 531 1943
fijoy.vadakkumpadan@sas.com

Joost Huiskens
SAS Institute, Inc.
+31 35 6996 831
joost.huiskens@sas.com